Inorganica Chimica Acta, *206* (1993) 141–153

The behavior of ferric protoporphyrin-IX in alkaline DMF

John W. Owens*, Johnny Robinson
Department of Chemistry, Southern University, Baton Rouge, LA 70813 (USA)

and Charles J. O'Connor
Department of Chemistry, University of New Orleans, New Orleans, LA 70148 (USA)

(Received July 7, 1992; revised November 12, 1992)

Abstract

The electronic and magnetic behavior of the azide adduct of ferric protoporphyrin-IX in neat and alkaline DMF has been examined. The electronic spectrum of this complex is different from that of other ferric porphyrins whether the porphyrin exists in a high or low spin state. The species has been characterized as Fe(3+)PPIX(DMF)(N_3). The electron spin resonance spectrum of this complex was examined in neat DMF from 298 to 4 K. These spectra are consistent with that expected for a system containing spin admixed $S = 5/2$ and $S = 1/2$ ground states, and, further suggests the possible existence of a spin equilibrium at low temperature. The behavior of hemin in a DMF/NaOH mixture was examined also. Results indicate that a ferric protoporphyrin dimer was formed, based on the appearance of a $\Delta M_s = 2$ transition. While neither the chloride ion nor imidazole was able to split the porphyrin dimer, the azide ion does, and at the same time maintains the existence of a spin admixed configuration.

Introduction

Ferric protoporphyrin-IX (Fig. 1(a)) is the prosthetic group for hemoglobin, myoglobin, cytochrome *c* and horseradish peroxidase. Its iron center is the active site for many heme proteins. Ferric protoporphyrin-IX chloride, commonly known as hemin (Fig. 1(b)), possesses two sites available for ligand coordination once the chloride ion has been removed. The nature of the ligand has been shown to affect the spin state of the five iron d electrons [3, 4]. When strong field ligands, e.g. cyanide, are attached, the d electrons pair and assume a low spin $^2T_{2g}$ configuration. Weak field ligands, e.g. chloride or fluoride, cause the d electrons to remain unpaired in a high spin $^6A_{1g}$ state.

Azide is a ligand which is known to be of intermediate strength, and when bonded to certain porphyrins, may cause the d electrons to assume more than one spin state depending on several factors, including temperature and the nature of the opposite axial ligand. A spin equilibrium between high and low spin states has been reported for azide complexes of ferric hemoglobin, HGB [5, 6], myoglobin, MGB [7] and hemeoctapeptide, H8PT [8]. Neya and Morishima [9] also characterized a spin equilibrium for the small ferric protoporphyrin-IX azide complex in dimethyl sulfoxide. Hemoglobin and myoglobin carry a ferrous ion in their natural state while H8PT and hemin are synthetic and contain a ferric ion near the center of the ring.

We now report an anomalous magnetic behavior for the azide adduct of ferric protoporphyrin-IX, PPIX, in dimethylformamide, DMF, based on variable temperature magnetic susceptibility and electron spin resonance studies. In particular, the azide adduct of ferric protoporphyrin-IX is shown here to exhibit a high spin configuration ($S = 5/2$) at room temperature but assumes an increasingly low spin configuration ($S = 1/2$) at temperatures near 4 K. The nature of the complex responsible for this behavior is believed to be a ferric protoporphyrin-IX–N_3–DMF complex. The magnetic behavior of this complex is compared with azide adducts of two other ferric complexes, hemoglobin and hemeoctapeptide.

We also compared the behavior of this azide adduct with the imidazole and cyanide adducts of ferric protoporphyrin-IX in alkaline DMF, a solvent prepared by mixing DMF with sodium hydroxide. The goal of this experiment was to gather more information about the electronic and magnetic behavior of iron porphyrin dimers in anhydrous solution containing the hydroxide ion; in particular, the behavior of the ferric protoporphyrin azide complex in this unique solvent.

*Author to whom correspondence should be addressed.

0020-1693/93/$6.00

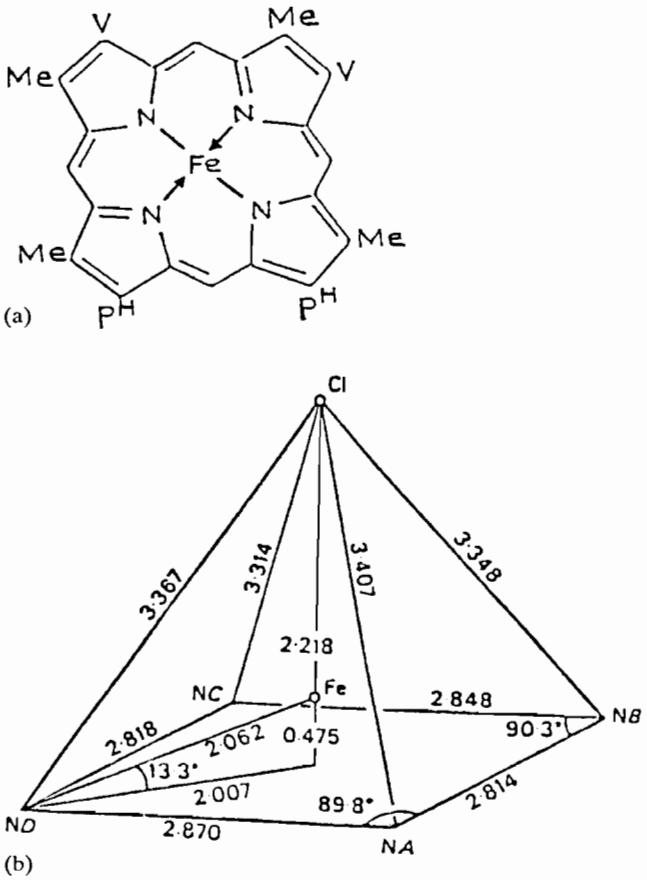

Fig. 1. (a) Schematic of ferric protoporphyrin-IX: Me = methyl, V = vinyl, P^H = propionic acid; taken from ref. 1. (b) Ferric protoporphyrin-IX chloride, from ref. 2.

Experimental

Electronic spectroscopy

Spectra were recorded with a Cary 14 spectrophotometer, using 1 cm quartz cells. Hemin was purchased from Sigma Chemical Company (St. Louis, MO) and used without further purification. Hemin solutions were prepared by dissolution in DMF at 3.3×10^{-5} M except in DMF/NaOH where the concentration was lowered to 2.2×10^{-5} M. DMF was purified and dried under nitrogen by double distillation over calcium oxide. Solutions of hemeoctapeptide, H8PT, were examined in a 50/50 vol./vol. ethylene glycol/40 mM phosphate buffer. H8PT was kindly provided by Dr Richard Kassner.

The azide adduct of Fe(3+)PPIX was prepared for electronic study by saturating a solution of hemin in DMF with sodium azide. A saturated solution of sodium azide in DMF is approximately 0.15 M. A spectrophotometric titration of a 3.3×10^{-5} M hemin solution with sodium azide in DMF (Fig. 2) was carried out at 635 nm using a Cary 14 spectrophotometer. Azide adducts of H8PT were prepared by dissolving the sodium salt in a 8.3×10^{-5} M solution of H8PT in a 50/50 vol./vol. ethylene glycol/40 mM phosphate buffer (spectra not shown because they were used only for comparison). Ligand numbers, where needed, were calculated using the following equation [10]

$$\log[A_0-A_\infty]/[A-A_\infty]=n\ \log[\mathrm{L}]+\log K \qquad (1)$$

where A_0 is the minimum absorbance before any ligand is added, A_∞ is the maximum absorbance at the highest ligand concentration, A represents absorbance values between the two extremes, K is the equilibrium constant, and n is the ligand number. A plot of log $[A_0-A_\infty]/[A-A_\infty]$ versus log[L] is shown in Fig. 3; no such titration of H8PT was needed since only one axial site was available for binding. Since the slope = 1.02, it is clear that only one azide ligand binds to ferric protoporphyrin. In this titration experiment, the azide concentration was varied as follows: 0.146, 0.293, 0.536, 1.172, 2.30, 4.688, 9.37 and 18.750 mM.

The electronic spectra of azide, imidazole and cyanide adducts of dimeric ferric protoporphyrin-IX were obtained by adding the ligand to a solution of Fe(3+)PPIX in alkaline DMF. Alkaline DMF was prepared by double distillation of DMF, followed by interaction with 100 g of NaOH pellets per 1000 ml DMF. This reaction was allowed to proceed for 24 h. The azide spectrum is shown in Fig. 4.

Rate studies were conducted on hemin concentrations of 1.79×10^{-4} M and ligand concentrations of 0.15 M in DMF, monitoring the beta band for the imidazole adduct (540 nm) and the charge transfer band for the azide adduct (635 nm). Rates were measured assuming pseudo first order kinetics whereby the ligand concentration was generally 1000 times that of the porphyrin.

Infrared spectroscopy

Room temperature spectra of the solid compounds sodium azide, ferric protoporphyrin-IX azide and hemin (Fig. 5) were obtained in KBr pellets on a Beckman 4260 spectrophotomcter, with a maximum resolution of 0.1 cm^{-1}. The powder form of ferric protoporphyrin-IX azide was prepared by mixing a saturated solution of the sodium salt in DMF and a saturated solution of ferric protoporphyrin-IX in DMF. This mixture was stirred overnight, the precipitate washed several times first with warm methanol to remove excess hemin and then with distilled water to remove excess sodium azide. After centrifugation, the powder was dried under vacuum.

Electron spin resonance

All ESR studies were carried out on a Varian E3 spectrometer at X-band, equipped with either a Varian liquid nitrogen variable temperature device or an Air Products helitran. Solutions of the azide adduct of ferric

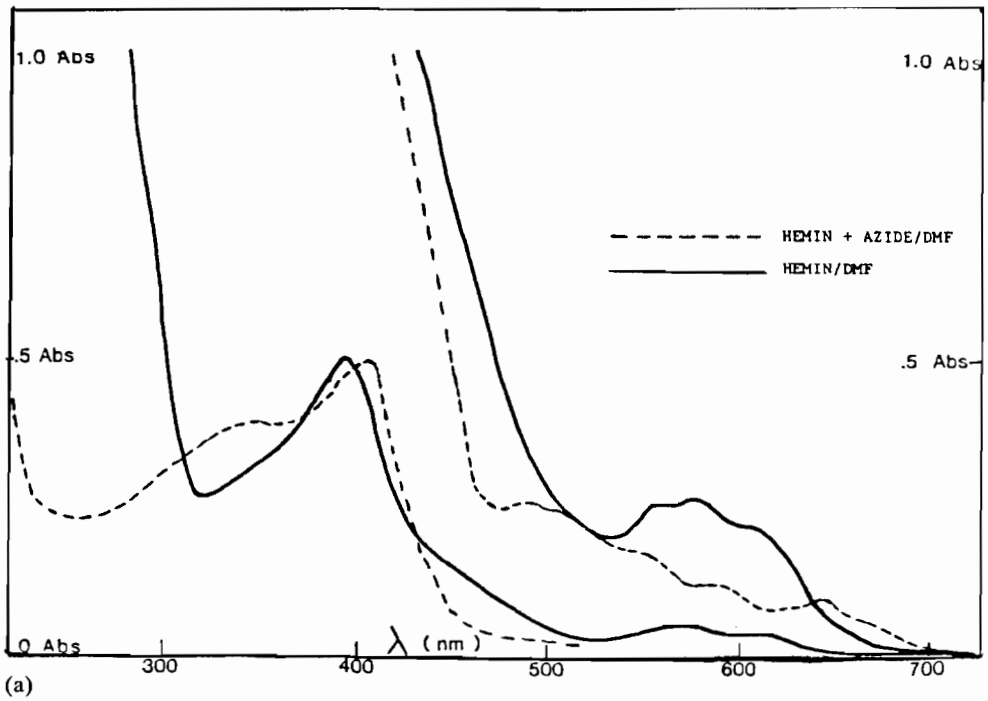

(a)

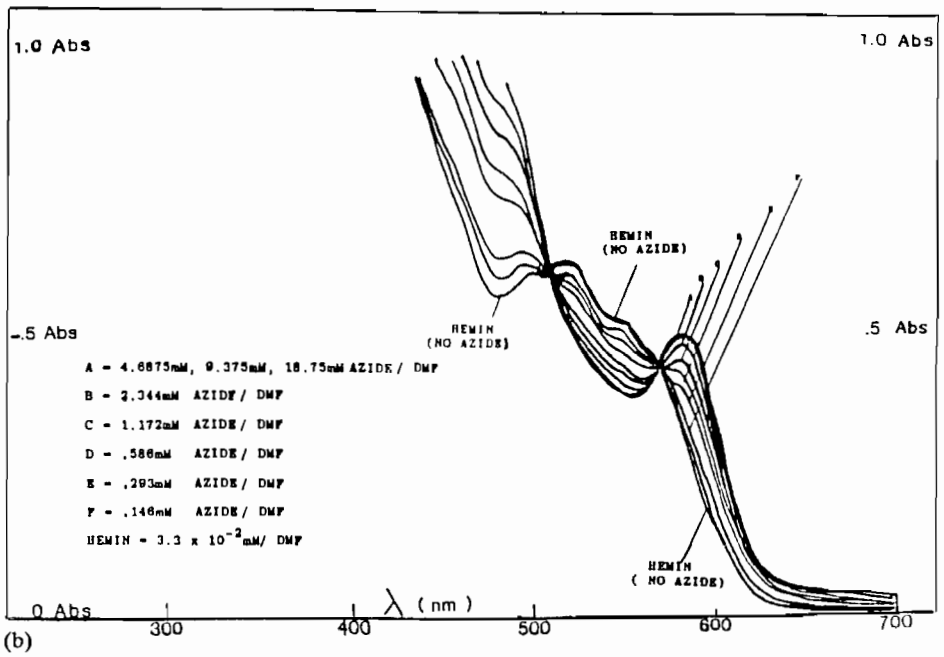

(b)

Fig. 2. Visible electronic spectrum of the spectrophotometric titration of hemin with azide in dimethylformamide (DMF) at 635 nm.

protoporphyrin-IX were prepared as described above, transferred to sterile quartz tubes, capped, and examined at 20 K intervals from 300 to 80 K (liquid nitrogen) and once at 4 K (helitran). Measurements between 80 and 4 K were not possible because of instrumental limitations. Overlapping variable temperature spectra of this complex are shown in Fig. 6. Solid samples of ferric protoporphyrin-IX chloride, ferric protoporphyrin-IX azide and hemeoctapeptide were also studied across this same temperature range.

The dimeric ESR studies of ferric protoporphyrin-IX azide in alkaline DMF were conducted by adding hemin to a solution of doubly distilled DMF which contained a saturated solution of sodium azide. This DMF solution had been kept over NaOH pellets for several days. Spectra are shown in Fig. 7.

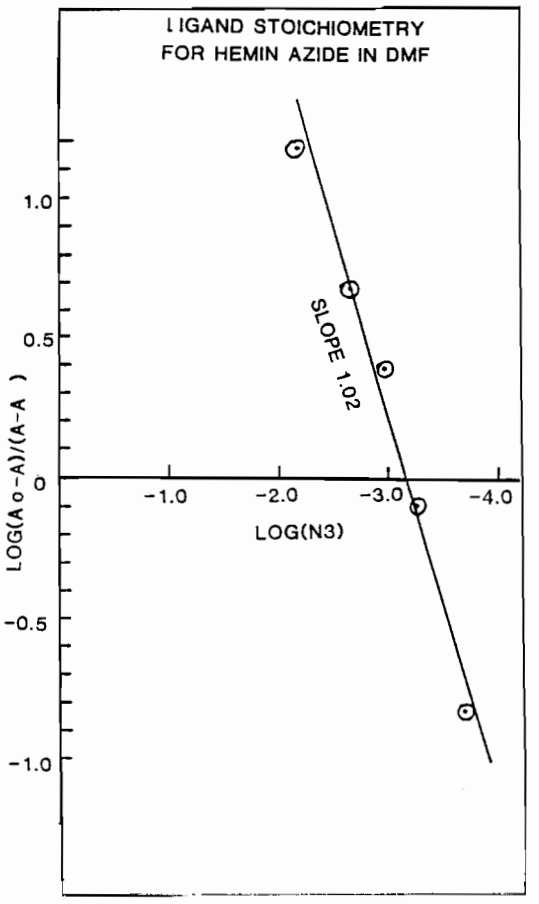

Fig. 3. Ligand number determination for the spectrum shown in Fig. 2. A plot of $\log[N_3^-]$ vs. $\log[A_0-A_\infty]/[A-A_\infty]$.

All g values were determined by comparison with DPPH, $g_1=g_2(H_2-H_1)$, and the system was periodically checked using both DPPH and a gauss meter.

Crystal field measurements

The quantification of tetragonal, rhombic, zero field splitting and orbital energies was carried out using a method outlined by Taylor [11]. According to this method, the d orbitals are arranged as shown below where only a perturbation of the t_{2g} orbitals (d_{xy}, d_{xz}, d_{yz}) is shown as the symmetry is lowered. Taylor's method assumes that the e_g orbital set, e.g. d_{z^2} and $d_{x^2-y^2}$, are completely isolated from the t_{2g} set. This method is therefore not valid for five-coordinate complexes nor six-coordinate high spin complexes. Under octahedral symmetry, all three t_{2g} orbitals are degenerate in energy. When there is an axial distortion and the symmetry is lowered to D_{4h}, this degeneracy is removed and the d_{xy} orbital is lowered in energy while the d_{xz} and d_{yz} orbitals are raised in energy, assuming a positive axial distortion.

The energy separation between the doubly degenerate d_{xz} and d_{yz} orbitals and the non-degenerate d_{xy} orbital is a measure of the tetragonal splitting, designated here as Δ. If there is a further lowering of symmetry by an in-plane mechanism, the symmetry is lowered from D_{4h} to D_{2h}, which removes the remaining energy degeneracy of the d_{xz} and d_{yz} orbitals while not affecting the energy of the d_{xy} orbital. The energy separation between the d_{xz} and d_{yz} orbitals is now a measure of the rhombic splitting, designated here as V. The electronic configuration of the low spin ferric complex is $d_{xy}^2 d_{xz}^2 d_{yz}^1$. When the single electron is allowed to rotate freely about its axes, spin orbit coupling and the rhombic field operator mixes in the E′ and the E″ states, such that the degenerate partners of each orbital, $m_s=\pm 1/2$ are no longer pure. Consequently, the wave functions which describe the degenerate partners of an orbital can be written as:

$$|+> = a|d_{yz}^+> - ib|d_{xz}^+> - c|d_{xy}^->$$

$$|-> = -a|d_{yz}^-> - ib|d_{xz}^-> - c|d_{xy}^+>$$

where a, b and c are mixing coefficients. If the Zeeman operator, $\mathscr{H}_{sp}=BH(\vec{L}_i+2\vec{S}_i)$, is applied to these functions (where B is the Bohr magneton, H is the applied field, $\vec{S}$ and $\vec{L}$ are the spin and orbital angular momentum operators, respectively, and $i=x$, y or z) and the equation, $\Delta E_i=g_iBH$ is used, the relationship between the mixing coefficients and the principal g values can be obtained

$$a=(g_z+g_y)/4p$$

$$b=(g_z-g_x)/4p$$

$$c=(g_y-g_x)/4p$$

where

$$p=(g_z+g_y+g_x)/2$$

The result of these equations assumes that the product $g_zg_yg_x$ is positive for $a=1.0$ and that there be no covalent bonding. Taylor's method is therefore only a first order approximation of the energy of these orbitals, since there is no attempt made to account for orbital reduction which might arise from spin orbit coupling or covalent bonding effects.

Once the coefficients were determined, they were used to obtain the energies of the d_{xz}, d_{yz} and d_{xy} orbitals by solving the determinant below

$$\begin{array}{c|c|c} |d_{yz}^+> & |d_{xz}^+> & |d_{xy}^->\\ \hline |d_{yz}^-> & |d_{xz}^-> & |d_{xy}^+> \end{array}$$

$$\lambda\cdot\begin{bmatrix} 0 & i/2 & -i/2 \\ -i/2 & -A & i/2 \\ -i/2 & -i/2 & -B \end{bmatrix}\begin{bmatrix} a \\ -ib \\ -c \end{bmatrix} = E\begin{bmatrix} a \\ -ib \\ c \end{bmatrix}$$

whose solution presents three secular equations

$$A=E(d_{xz})=g_x/(g_z+g_y)+g_y/(g_z-g_x)$$

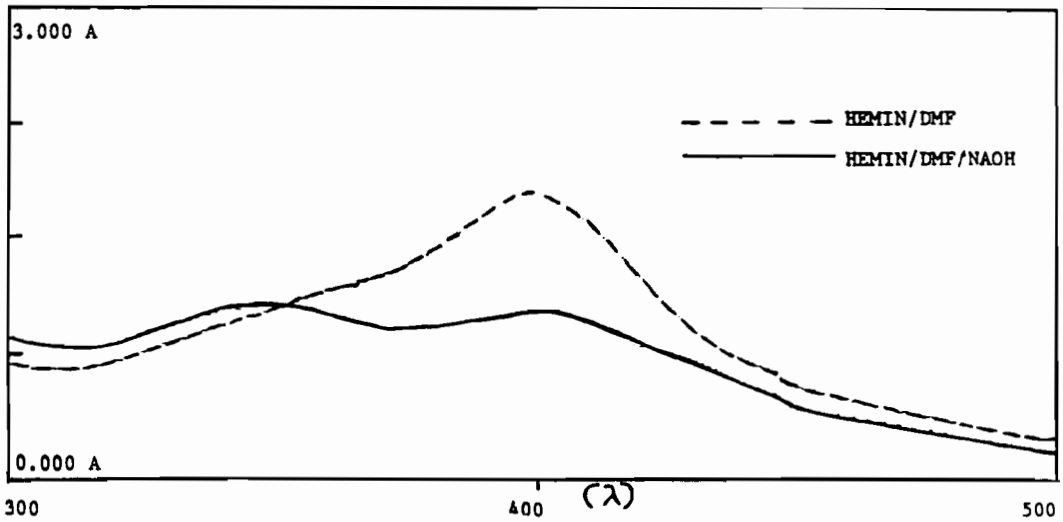

(a)

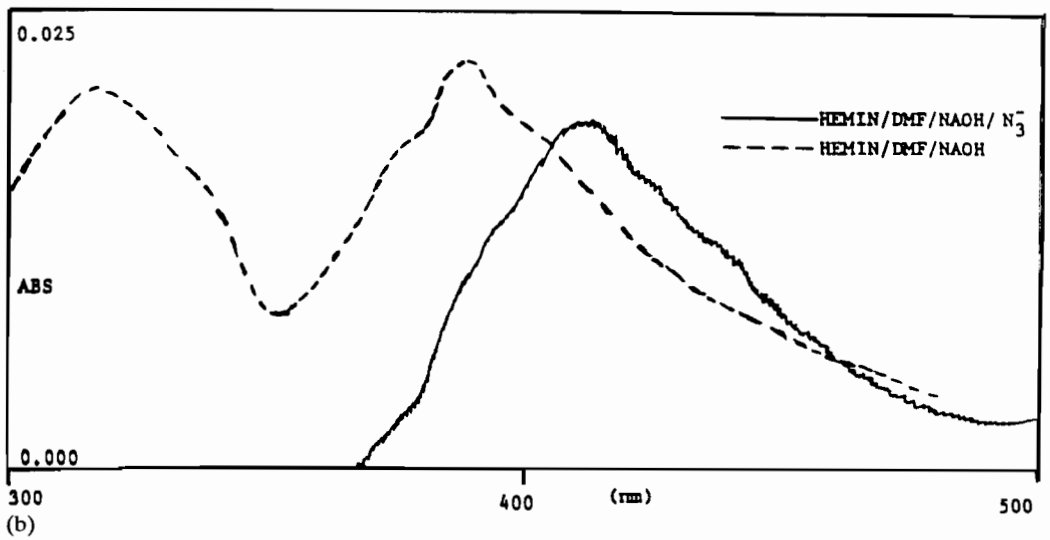

(b)

Fig. 4. (a) Absorption spectrum of 3.3×10^{-5} M hemin in DMF and in a saturated mixture of NaOH and DMF. (b) 1.02×10^{-5} M hemin in DMF and in a saturated mixture of NaOH and DMF.

$$B = E(d_{xy}) = g_x/(g_z+g_y) + g_z/(g_y-g_x)$$

$$E = E(d_{yz}) = g_x/(g_z+g_y) - 1/2$$

whose energies are in units of $\lambda = 400$ cm^{-1}, the spin orbit coupling constant.

For Taylor's model, the d_{yz} orbital lies lowest and the d_{xy} orbital lies highest in energy. The tetragonal splitting, Δ, is readily seen to be just $B-A/2$ and the rhombic splitting is readily seen to be just A. The energy of the orbitals are all relative to E, the energy of the d_{yz} orbital. In a conventional energy diagram, the energies of these orbitals would be reversed with the d_{yz} orbital highest in energy. The ESR g values, mixing coefficients, tetragonal and rhombic splitting parameters, and orbital energies for all of the complexes examined here are shown in Tables 1 and 2.

Results and discussion

The electronic spectrum of Fe(3+)PPIX in DMF is shown in Fig. 2(a). The Soret band is present at 396 nm, with four other bands appearing in the visible region at 550, 570, 600 and 620 nm (see Table 3). No band was observed at 500 nm. The electronic profile of high spin ferric porphyrins, $S = 5/2$, has been reported to exhibit an intense Soret band in the UV region, and two other bands in the visible region near 500 and 540 nm [15]. These two latter bands are sometimes called the β and α bands, respectively [16]. The positions

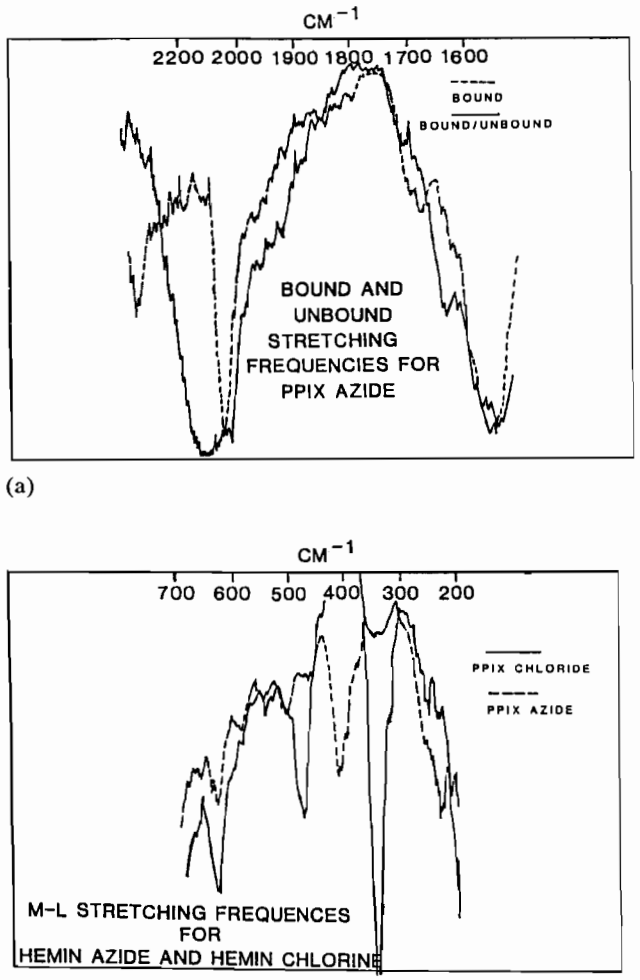

Fig. 5. (a) IR spectrum of hemin, Fe(3+)PPIX(Cl) and the azide adduct; a comparison of the Fe–L stretching frequencies. (b) A comparison of the asymmetric internal stretching frequencies for unbound versus bound azide.

of these two bands shift to approximately 540 and 570 nm in low spin ferric porphyrins with spin $S = 1/2$.

The absence of a band at 500 nm in the hemin spectrum, whose d orbitals are known to assume a high spin configuration, could indicate the presence of a small amount of dimethylamine in DMF. Dimethylamine is a ligand which traditionally produces a low spin complex when coordinated to ferric porphyrins. DMF is known to breakdown into dimethylamine over a long period of time. The electronic spectrum of such a Fe(3+)PPIX/DMF/dimethylamine system would be expected to exhibit either a mixture of high and low spin states or an exclusively low spin spectrum [17], depending on the amount of amine present. It was later found, however, that the band near 500 nm was either absent or barely observable even when hemin was dissolved in fresh DMF. It is therefore not likely that dimethylamine was present.

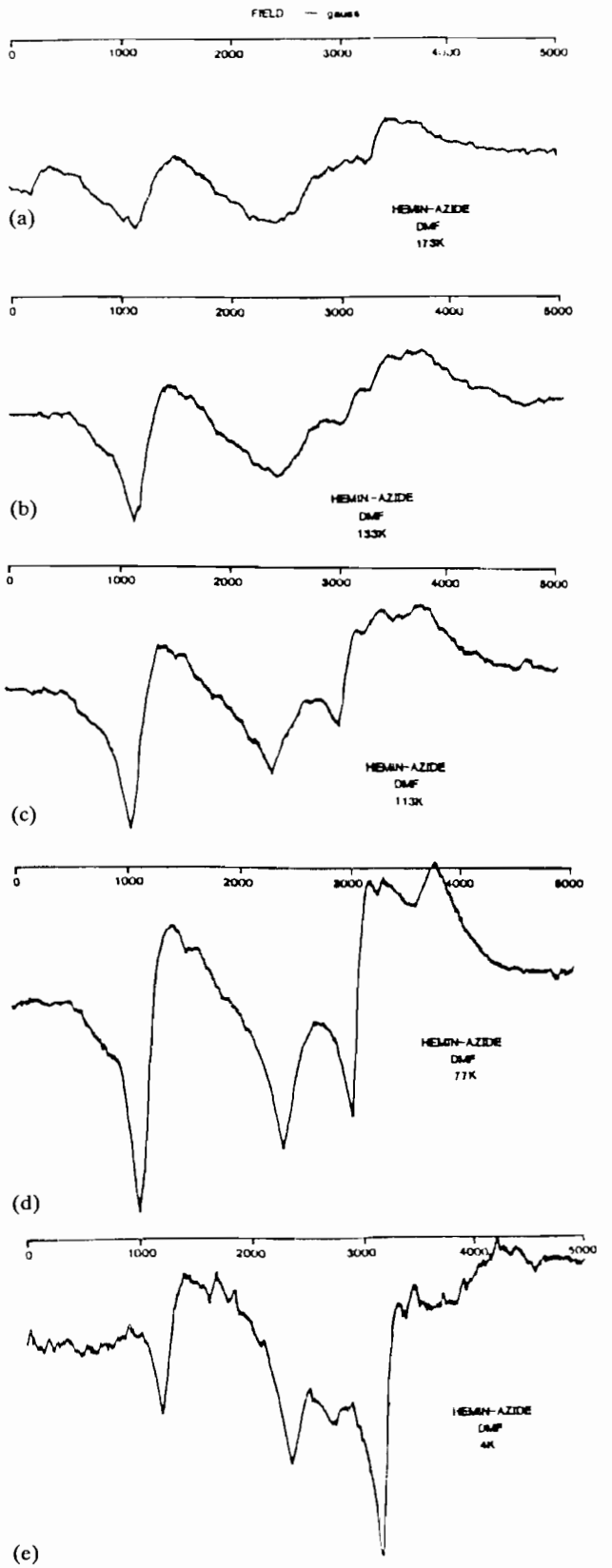

Fig. 6. Overlapping electron paramagnetic resonance spectra for Fe(3+)PPIX(DMF)(N_3) at (a) 177, (b) 133, (c) 113, (d) 77 and (e) 4 K.

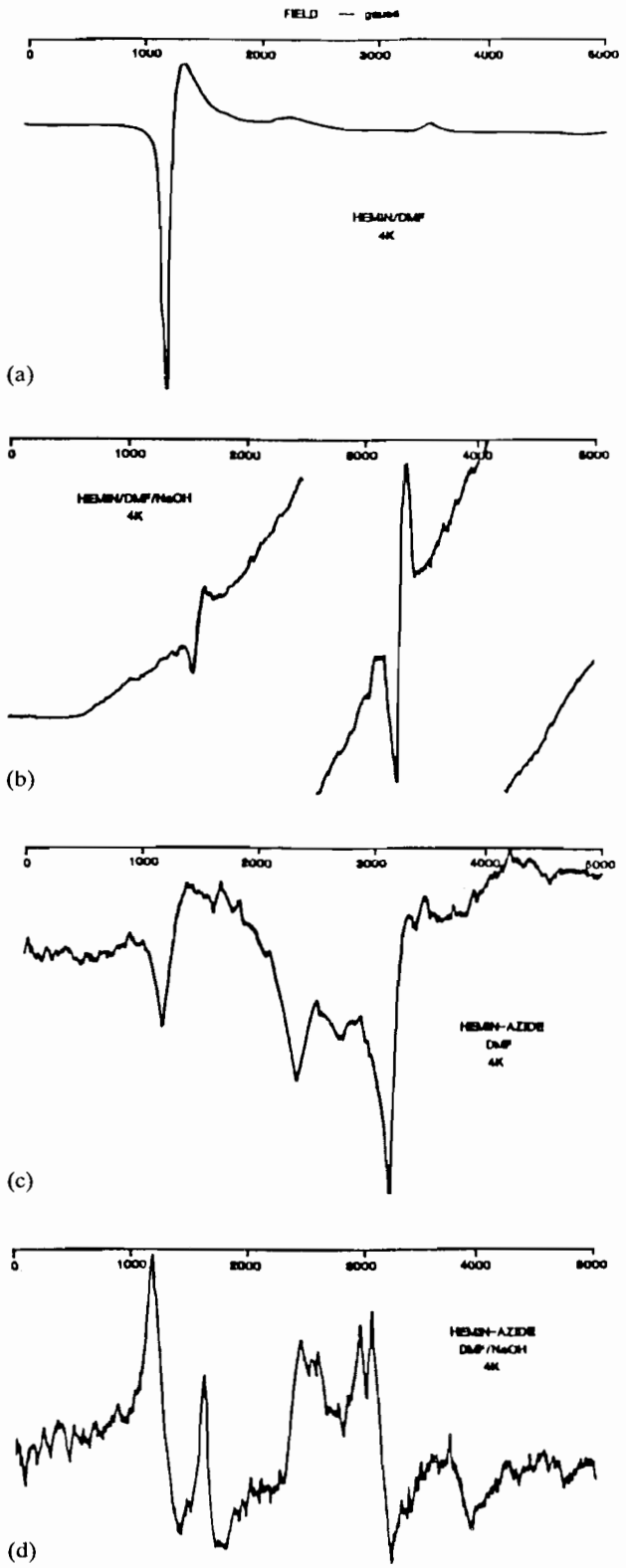

Fig. 7. A comparison of the electron paramagnetic resonance of: (a) Fe(3+)PPIX(Cl), which is hemin, in neat DMF; (b) Fe(3+)PPIX(Cl) in a saturated solution of NaOH pellets in DMF; (c) Fe(3+)PPIX(DMF)(N_3) in neat DMF; (d) Fe(3+)PPIX(DMF)(N_3) in a saturated solution of NaOH pellets in DMF; at 4 K.

Some transition metals are able to catalyze a decomposition of DMF to dimethylamine. Therefore, it is possible that the apparent low spin character in the spectrum of hemin in DMF could be attributed to the presence of trace amounts of one or more transition metals. Another possibility is the presence of a small amount of water in DMF. When hemin is dissolved in such a wet mixture a complicated spin system could result [17], producing an electronic spectrum containing both high and low spin bands.

When this hemin/DMF solution was examined by electron spin resonance over the temperature range 300–4 K, only a high spin species was observed (see Fig. 7). There was no evidence to support the existence of a low spin component over this temperature range. Results of the electronic and magnetic data can only be explained by assuming that the hemin/DMF system does indeed exist as a predominantly high spin species with the usual marker at 500 nm being either absent or severely depressed. The exact reason for this absence is not known.

In an effort to find out more about the absence of the 500 nm marker, PPIX was studied in DMSO, pyridine and methanol. The latter two solvents have been reported to be non-coordinating [18]. A band occurring near 500 nm was observed in all of these solvents. DMSO is even more hygroscopic than DMF, but, when hemin was examined in DMSO, only those bands associated with the high spin species appeared. Therefore, it is also unlikely that the unique hemin/DMF spectrum can be attributed to the presence of water in the solvent.

Conductivity measurements have shown that the chloride ion does not dissociate from ferric protoporphyrin in DMF [17]. This same study also concluded that hemin will not associate in DMF. Kadish has reported the existence of an Fe(3+)TPP(DMF)(Cl) species in electrochemical studies (TPP = tetraphenylporphyrin), suggesting the coordination of the DMF molecule [19]. Lamar and Zorbrist have also reported the coordination of both DMSO and DMF to Fe(3+)TPP iodide at both axial sites [20]. When all of these reports are taken together, they suggest that the species responsible for the production of the electronic and magnetic spectra described above can best be represented as Fe(3+)PPIX(DMF)(Cl). We believe that it is the coordination of DMF to hemin which is responsible for the presence of the low spin character in its electronic spectrum, and that it is the coordination of DMF which prevents the appearance of the high spin marker near 500 nm.

The coordination of the azide ligand to ferric protoporphyrin-IX in DMF is an unusually difficult and comparatively slow reaction to drive to completion. The Soret band, appearing at 396 nm in hemin solution,

TABLE 1. Electron spin resonance parameters for several ferric porphyrins containing azide

Complex	g Values	Reference	Mixing coefficients	Maximum unpaired spin density
PPIX azide	2.80, 2.10, 1.74	this work	0.975, 0.211, 0.072	d_{yz}
H8PT azide	2.78, 2.14, 1.70	12	0.969, 0.213, 0.087	d_{yz}
HMGB azide	2.80, 2.22, 1.74	13	0.977, 0.210, 0.097	d_{yz}
CYTC azide	2.72, 2.24, 1.73	14	0.976, 0.195, 0.100	d_{yz}

TABLE 2. Crystal field parameters for ferric porphyrins containing azide ligands

Complex	$E(d_{xz})$[a]	$E(d_{xy})$	V[b]	Δ[c]	V/Δ
PPIX azide	2.34	8.13	936	2784	0.336
H8PT azide	2.33	6.66	931	2198	0.423
HMGB azide	2.40	5.94	959	1896	0.506
CYTC azide	2.59	5.70	1036	1762	0.588

[a]Energies are in 400 cm^{-1}. [b]V = rhombic splitting. [c]Δ = tetragonal splitting.

shifts to the red and appears at 405 nm when the azide ion coordinates; the band originally present at 550 nm in hemin solution shifts to 535 nm when the azide ligand coordinates; the band located at 570 nm in the hemin solution remains unshifted when the azide ligand coordinates. A new band appears at 500 nm (see Table 3). The band near 500 nm is not very intense in the Fe(3+)PPIX(DMF)(N_3) complex but it is clearly observable, as shown in Fig. 2(b).

New bands at 500 and 535 nm in the spectrum of Fe(3+)PPIX(DMF)(N_3) are indicative of a high spin component, while the bands located at 535 and 570 nm indicate the existence of a low spin component. A similar high spin/low spin behavior has been reported for the azide adduct of Fe(3+)PPIX dissolved in DMSO [9]. The charge transfer band originally present at 620 nm in hemin shifts to 635 nm and becomes more intense when the azide ion coordinates.

Results of a spectrophotometric titration at 635 nm of Fe(3+)PPIX with azide in DMF yielded a ligand number of 1.02 (Fig. 3). The IR spectrum of the solid complex, Fe(3+)PPIX(N_3), in KBr pellets also showed that the azide group was bound to Fe(3+)PPIX. The ν(Fe–Cl) asymmetric stretching frequency of hemin appeared at 357 cm^{-1}, but the ν(Fe–N_3) asymmetric stretch appeared near 412 cm^{-1} in the azide adduct [21]. Attempts to characterize a solution spectrum of Fe(3+)PPIX(DMF)(N_3) by IR spectroscopy were unsuccessful because of the presence of a high concentration of unbound azide. The ratio of azide to porphyrin in this solution was nearly one thousand. This always produced an intense and broad internal asymmetric stretch for unbound azide which dominated the region where the bound azide frequency would be expected to occur (see Fig. 5). The binding of azide to hemin requires a large excess of azide, much more so than that required to coordinate imidazole or cyanide ions.

The formation of Fe(3+)PPIX(DMF)(Cl) is assumed to be diffusion controlled under the conditions of this experiment. The ligand addition mechanism is assumed to proceed as follows

TABLE 3. Electronic absorption parameters for ferric protoporphyrin complexes (absorptivities $\times 10^4$ are given in parentheses)[a]

Complex in DMF[b]	Band positions (nm)					
Hemin	350 (3.424)	396 (5.652)	550 (0.500)	570 (0.545)	600 (0.470)	620 (0.379)
Hemin/NaOH	350 (5.114)	386 (5.114)	550 (0.636)	570 (0.636)	600 (0.509)	620 (0.509)
Hemin/azide	350 (1.818)	405 (2.282)	500 (0.400)	540 (0.284)	570 (0.222)	635 (0.182)
Hemin/azide/NaOH[c]		413 (0.115)			570 (0.009)	
Hemin/DMSO		402 (6.666)	500 (0.304)	540 (0.154)		610 (0.242)
Hemin/azide/DMSO		410 (3.030)	500 (0.242)	540 (0.242)	570 (0.180)	630 (0.254)

[a]Solutions are 3.3×10^{-5} M except in NaOH where the concentrations are 2.2×10^{-5} M. [b]Solvent is DMF unless otherwise indicated. [c]Concentration is 1.0×10^{-5}M because of the limited solubility of sodium azide in DMF/NaOH.

$$Fe(3+)PPIX(Cl)+DMF \longrightarrow Fe(3+)PPIX(DMF)(Cl) \quad (2)$$

$$Fe(3+)PPIX(DMF)(Cl)+N_3^- \longrightarrow Fe(3+)PPIX(DMF)(N_3)+Cl^{-1} \quad (3)$$

where eqn. (2) is assumed to be diffusion controlled. For azide addition, the disappearance of Fe(3+)-PPIX(DMF)(Cl) is governed by the following rate equation

$$-d[Fe(3+)PPIX(DMF)(Cl)]/dt = k_1[Fe(3+)PPIX(DMF)(Cl)][N_3^-] - k_{-1}[Fe(3+)PPIX(DMF)(N_3)][Cl^-] \quad (4)$$

$$= k_{obs}[Fe(3+)PPIX(DMF)(Cl)] - k_{-1}[Fe(3+)PPIX(DMF)(N_3)][Cl^-] \quad (5)$$

If the ligand concentration significantly exceeds that of the porphyrin, where $[N_3^-] \gg [Fe(3+)PPIX-(DMF)(Cl)]$, then eqn. (5) can be reduced to

$$k_{obs} = k_1[N_3^-] \quad (6)$$

We measured this rate constant at 535 nm in DMF assuming pseudo first order kinetics. It has been shown that most nitrogen-containing ligands binding to porphyrins can be kinetically characterized this way [22]. The rate constant, k_{obs}, measured 42.06 s^{-1}. The ligand concentration was 1.50×10^{-1} mol/l, about 1000 times that of the hemin, 1.79×10^{-4}. k_1 was found to be 2.80×10^2 M^{-1} s^{-1}. The equilibrium constant for the reaction, $K=1.259\times10^4$, was calculated from the spectrophotometric titration of azide with Fe(3+)PPIX. Using these values for k_1 and K, k_{-1} measured 2.16×10^{-2} M^{-1} s^{-1}, a value which proves that the equilibrium in eqn. 2 lies far to the right.

Figure 6 shows the overlapping variable temperature electron spin resonance spectra of Fe(3+)PPPIX-(DMF)(N_3) from room temperature to 4 K. Because of instrument limitations no experiments were performed below 4 K. Near room temperature, this complex exhibits no visible ESR absorption, presumably due to a significant spin lattice relaxation [23]. Inspection of overlapping spectra occurring between 173 and 77 K shows a sequential build-up of the high spin species with g values present at 6.0 and 2.0. These anisotropic g values are consistent with an axially distorted tetragonal complex with a $^6A_{1g}$ ($S=5/2$) ground state in which $g_x=g_y\neq g_z$ [24]. The peak occurring at $g=6.0$ represents the contribution to g from the xy plane and the peak occurring at $g=2.0$ represents the contribution to g from the z axis. The increasing intensity at low temperature is brought about by an increase in the lifetime of the excited states of the electrons.

At 4 K, Fig. 6 contains a spectrum which is decidedly low spin in character, with the high spin component still present but much less intense. At this temperature, the ESR spectrum contains g values at 1.74(g_x), 2.10(g_y) and 2.80(g_z) and is associated with a rhombic anisotropic system where $g_x\neq g_y\neq g_z$. This labeling system follows that originally proposed by Blumberg [25]. This spectrum is consistent with a system whose ground state is predominantly low spin, $^2T_{2g}$ ($S=1/2$). The low field high spin component at $g=6.0$, although present throughout, is much less intense at 4 K.

We first reported an unusual spin state for this complex in 1984 based on electron spin resonance measurements at 77 K and on electrochemical studies [26]. At this time we characterized this system as mixed spins, $S=5/2$ and $S=1/2$. A system containing admixed spin states would be expected to exhibit both states over a wide temperature range (unless the two states are frozen in at some higher temperature and continue to coexist over a lower temperature range) whereas a system containing a true spin equilibrium would be expected to exhibit one spin state over one temperature range and a second spin state over a different temperature range, with a spin crossover occurring over a very narrow temperature range.

Our results clearly indicate that the Fe(3+)-PPIX(DMF)(N_3) complex is of mixed spins. This could be explained by assuming that the populations of these states are in thermal equilibrium, giving rise to the presence of both a low and high spin component. Because we don't have the instrumental capability to measure a temperature dependence on the spin populations; $[5/2]/[1/2]=\exp(\Delta G/kT)$, we cannot prove that this system contains a spin crossover. A variable temperature magnetic susceptibility analysis of this solution is currently underway utilizing a superconducting quantum interference device (SQID). That analysis should help to further characterize this unique complex.

Crystal field effects

Based on the ESR data, we have calculated ligand field parameters for several azidoporphyrins, in order to characterize properties common to all of them, utilizing a technique described by Taylor [11] for low spin d^5 systems involving the e_g and t_{2g} orbitals. These parameters are given in Tables 1 and 2. Taylor's scheme is explained in earlier publications [11, 26]. The tetragonal splitting can be measured as the separation between the d_{xy} and degenerate d_{xz}, d_{yz} orbitals [27] while the rhombic splitting is measured as the separation between the d_{yz} and d_{xz} orbitals (Fig. 8). All of the azide complexes in Tables 1 and 2 exhibit large tetragonal, Δ, and rhombic, V, distortions, with V/Δ ratios ranging from a maximum of 0.597 in the cytochrome azide complex to a low of 0.336 in the Fe(3+)PPIX

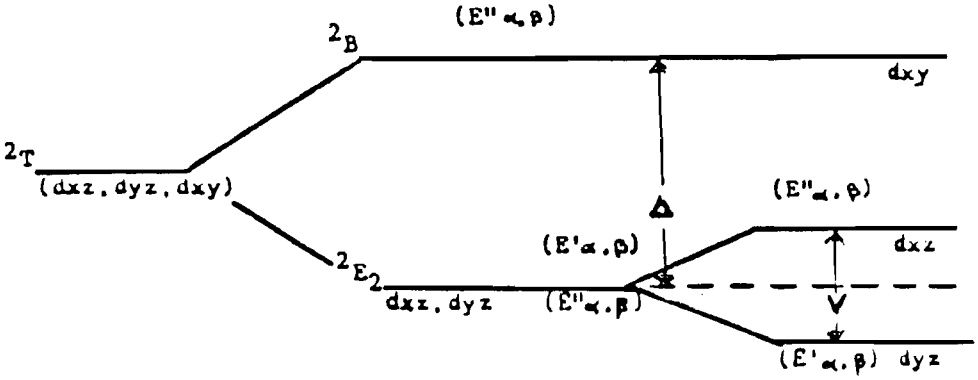

Fig. 8. The low spin $S=1/2$ orbital scheme for the $^2T_{2g}$ d^5 orbitals as applied by Taylor under the influence of spin orbit coupling and the tetragonal and rhombic field operators.

azide complex. The tetragonal distortion decreases systematically in the azido series: Fe(3+)PPIX> H8PT>HGB>CYCT, while the rhombic distortion generally follows the reverse order. This trend appears to be a reflection of protein environment. The degree of tetragonal splitting has previously been correlated with metal–ligand bond length [27].

Interpretation of the magnitude of the rhombic splitting in these complexes is more difficult to assess since the values are not significantly different, but it has been suggested that the degree of rhombicity is dependent on the placement of the metal relative to the porphyrin plane [28]. Results of X-ray crystallographic studies on low spin ferric complexes of hemoglobin and tetraphenylporphyrin [29, 30] do support this assumption, but care should be taken to avoid formulating a trend based on two data points. Because all of these azide complexes except cytochrome *c* have been reported to contain a spin equilibrium, it is reasonable to assume that the energy separation between the high and low spin ground states is similar in all these complexes [31].

The degree of energy separation between the ground states in porphyrins often serves as a marker for the existence of a spin equilibrium. Our calculations suggest that if a true spin equilibrium does exists in these ferric azide porphyrins, it must depend in some way on the degree of rhombic splitting.

Dimeric effects

ESR spectra of Fe(3+)PPIX and its azide adduct are shown in Fig. 7 at 4 K and g values are shown in Table 4. The electronic spectral of these complexes are shown in Fig. 4. When hemin is dissolved in DMF (Fig. 7(a)), its ESR spectrum is consistent with a high spin tetragonal system with g values occurring at 5.28, the perpendicular contribution, and at 1.93, the parallel contribution. A g value occurring at $g=5.28$ rather than at $g=6.0$ can be explained by assuming a quantum mechanical quartet admixture. These g values are associated with a monomer and derive from a $\Delta M_s=1$ transition in the lowest Kramer's doublet. The spectrum of hemin in alkaline DMF (Fig. 7(b)) is different; two peaks appear: one at low field, $g=3.99$ (H ~ 1500 gauss), and one at mid-field, $g=1.97$. The peak appearing at $g=3.99$ derives from a $\Delta M_s=2$ transition and is consistent with that reported for other dimeric porphyrins containing metals with $S=1/2$ ground states [32]. Based on a comparison of this system with other porphyrins, it is likely that this species can be described as a μ-oxo dimer. The existence of these dimers has been attributed to a coupling of the metal ions through the oxygen atom [32]. Coupling between metalloporphyrins through the hydroxide ion has also been reported for a high spin bis heme NaOH complex [33].

TABLE 4. Electron spin resonance parameters for complexes of ferric protoporphyrin-IX at 4 K

Complex in DMF	g Values
Hemin	5.28, 1.93
Hemin/NaOH	3.99, 1.97
Hemin/azide	5.12, 2.80, 2.10, 1.74
Hemin/azide/NaOH	5.27, 3.99, 2.76, 2.10, 1.99, 1.71
Hemin/imidazole/NaOH	3.99, 1.97
Hemin/cyanide/NaOH	3.99, unresolved peaks

It is possible to observe a $\Delta M_s=2.0$ transition in ESR spectra but it has never been observed in ferric μ-oxo porphyrin dimers. Presumably the absence of an ESR signal in these μ-oxo dimers is due to the rather strong antiferromagnetic coupling between the unpaired ferric d electrons. As far as we can tell, this is the first report of ESR activity in a ferric μ-oxo porphyrin dimer. Until now, however, no one has studied hemin solutions in this unique DMF/NaOH solvent.

When Fe(3+)PPIX(N_3) was prepared in DMF (Fig. 7(c)), several peaks appeared with g values of 5.12, 2.76, 2.10 and 1.71. Such a spectrum is consistent with a spin admixed $S=5/2$ and $S=1/2$ system. The electronic

spectrum of this solution supported the presence of a high spin/low spin equilibrium. When Fe(3+)PPIX(N_3) was prepared in alkaline DMF (Fig. 7(d)), its ESR spectrum was similar to that in Fig. 7(c) except that a new signal appeared at $g=3.99$. The appearance of this peak suggested that two species were present: dimeric hemin and the spin admixed complex of Fe(3+)PPIX(DMF)(N_3). The presence of an electronic band at 413 nm in this complex in alkaline DMF clearly demonstrated the coordination of the azide ion (Fig. 4), although the location of this band is about 8 nm farther to the red than in neat DMF. For comparison, Fe(3+)PPIX azide was examined at 4 K in methanol, a protic polar solvent, and in DMSO, an aprotic polar solvent (Fig. 9). Both spectra are consistent with that for a typical high spin species with g values present near 6.0 and 2.0. There was no evidence to suggest the presence of a dimeric species at low field in either of these two solvents.

We also examined the chemistry between imidazole and Fe(3+)PPIX in alkaline DMF (Fig. 10(a)). The ESR spectrum was remarkably similar to that for hemin in alkaline DMF, although there is some evidence to suggest the coordination of imidazole. There was little evidence to support the presence of a monomeric species; however, we assumed that the coordination of imidazole necessarily caused the dimer to split, although not necessarily stoichiometrically. When cyanide was mixed with hemin in this alkaline DMF solution, ESR resonance was observed in anisotropic form centered about $g=2.0$ (Fig. 10(b)), suggesting the coordination of the cyanide ion. These g values, however, were not well resolved. Cyanide is generally considered a stronger π acid ligand than imidazole and is recognized as a good electron acceptor. We assume that the π acceptor ability of the cyanide ion allows for an easier coordination to iron dimers than imidazole.

Although imidazole is a better π acceptor than azide, it apparently does not coordinate this particular iron porphyrin dimer as easily as azide and cyanide ions. The chloride ion produced no effect on the dimer. The imidazole ligand could be either too big, dimerized in DMF, or too structurally altered by the solvent to interact with the dimer. There is a precedent for this kind of behavior [34]. The azide ion is neither a strong base nor a good π acid ligand, but is nevertheless better able to split the dimer than imidazole or cyanide.

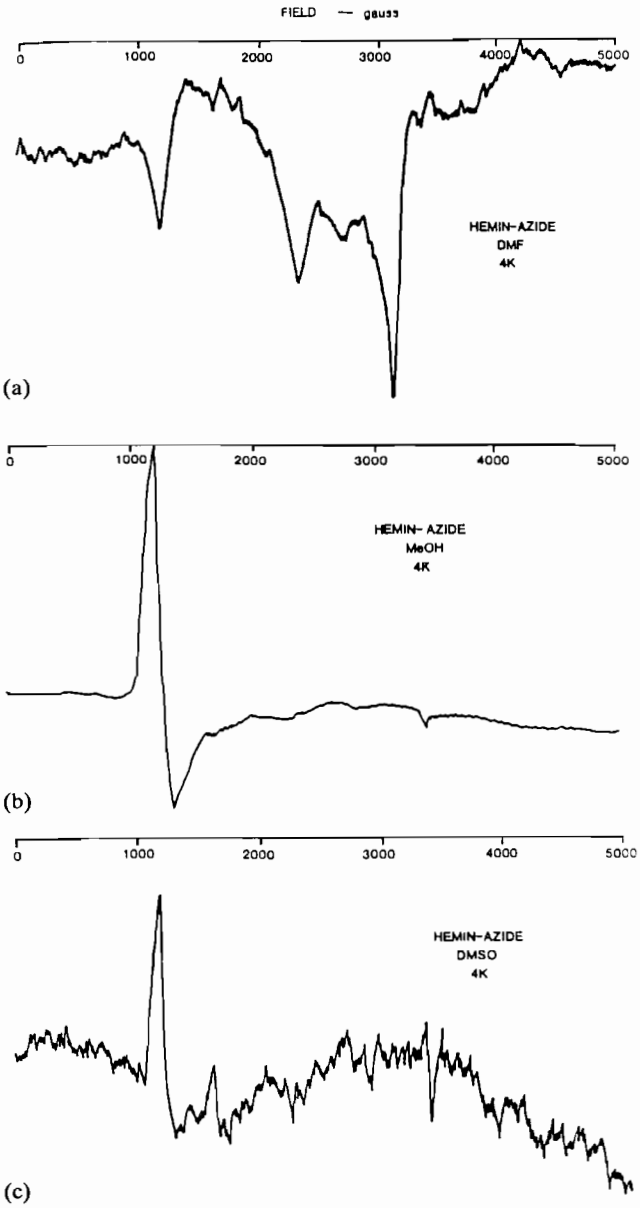

Fig. 9. A comparison of the behavior of ferric protoporphyrin-IX azide adducts in DMF (a), methanol (b) and DMSO (c) at 4 K.

Conclusions

An examination of the electronic and magnetic behavior of the azide adduct of Fe(3+)PPIX and several other ligands in DMF have shown that the azide adduct behaves uniquely. The azide adduct presents both a unique electronic and ESR spectrum. The electronic spectrum has been characterized as a mixture of high spin and low spin states. The spectrum of Fe(3+)PPIX in DMF is very different from that of other high spin iron porphyrins in various other solvents regardless of the solvent's polarity or hygroscopic affinity. When azide coordinated to this complex, the species was characterized as Fe(3+)PPIX(DMF)(N_3).

Utilizing ESR, crystal field parameters for Fe(3+)PPIX(DMF)(N_3) were calculated from Taylor's matrices and compared to crystal field parameters for other azidoporphyrins exhibiting spin equilibria. The

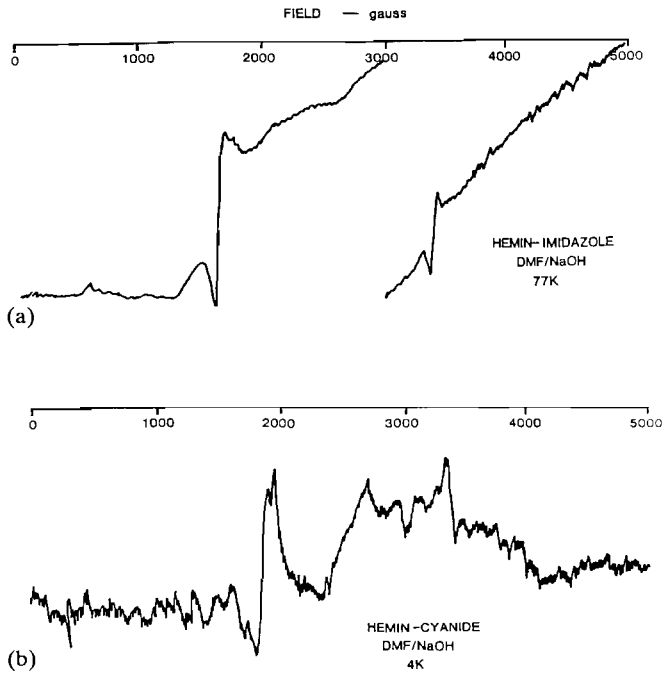

Fig. 10. ESR spectrum of imidazole (a) and cyanide (b) in NaOH/DMF at 4 K.

existence of the spin equilibrium in these complexes was suggested to be dependent on crystal field effects.

ESR spectra of the ferric protoporphyrin azide complex in DMF over the temperature range 298–4 K exhibited a classic spin admixed system with $S=5/2$ and $S=1/2$ ground states. A spin crossover could not be characterized but was strongly implied.

The behavior of Fe(3+)PPIX(Cl), Fe(3+)PPIX-(DMF)(N_3) and two other adducts of Fe(3+)PPIX was examined in alkaline DMF utilizing ESR at 4 K. All of these complexes exhibited a classic $\Delta M_s=2.0$ transition with a g value of 3.99. This is the first report of an ESR active ferric porphyrin μ-oxo dimer.

The binding affinity of ligands for these metalloporphyrins does not appear to be a function of basicity nor π acid ability. Neither cyanide, a good π acid ligand, imidazole, nor azide ligands were able to completely split the Fe(3+)PPIX/DMF/OH dimer. Evidence from the ESR spectra did suggest that these ligands coordinated the iron center. We assume then that this porphyrin dimer must be split to some extent by the coordination of these ligands. It is not likely that iron assumes a seven-coordinate capability. The ESR profiles, however, provide clear evidence of dimer splitting only in the case of the azide bound porphyrin complex. Coordination of imidazole and cyanide ions to this dimer produced much less splitting. The enhanced ability of the azide ion to split this dimer may be related to the existence of admixed spin states.

Acknowledgements

The research for this manuscript was supported in part by the National Institutes of Health under grant no. S06GM08025-20. The authors thank Dr Richard Kassner for suppling hemeoctapeptide, Dr Ray Sweaney for his help with the IR spectra and solvent purification, and Drs Frederick Christian, Earl Doomes and Robert Miller for their support and guidance throughout the preparation of this manuscript.

References

1 K. Smith (ed.), *Porphyrins and Metalloporphyrins,* Elsevier, Amsterdam, 1975, pp. 11–15.
2 D. F. Koenig, *Acta Crystallogr., 18* (1965) 663.
3 W. S. Caughey, in I. Eichhorn (ed.), *Inorganic Biochemistry,* Vol. 2, Elsevier, Amsterdam, 1973, p. 797.
4 M. Weissbluth, *Hemoglobin: Cooperativity and Electronic Effects, Molecular Biology, Biochemistry and Biophysics Series,* Vol. 15, Springer, New York, 1974.
5 T. Lizuka and M. Kotani, *Biochim. Biophys. Acta, 194* (1969) 351.
6 J. O. Alben and L. Fager, *Biochemistry, 11* (1972) 842.
7 J. Beetlestone and P. George, *Biochemistry, 3* (1964) 707.
8 R. D. Kassner and Y. Huang, *J. Am. Chem. Soc., 103* (1981) 4927.
9 S. Neya and I. Morishima, *J. Am. Chem. Soc., 104* (1982) 5648.
10 H. E. Bent and C. L. French, *J. Am. Chem. Soc., 63* (1941) 568.
11 C. P. S. Taylor, *Biochim. Biophys. Acta, 491* (1977) 137.
12 J. W. Owens, C. J. O'Connor and R. D. Kassner, *Inorg. Chim. Acta, 151* (1988) 107.
13 J. F. Gibson and D. J. E. Ingram, *Nature (London) 180,* (1957) 29.
14 J. Peisach and J. Blumberg, *J. Biol. Chem., 262* (1977) 574.
15 (a) A. S. Brill and R. J. P. Williams, *Biochem. J., 78* (1961) 246; (b) R. J. P. Williams and D. W. Smith, *Struct. Bonding (Berlin), 7* (1970) 1.
16 (a) M. Gouterman, H. Kobayashi and M. Zerner, *Theor. Chim. Acta (Berlin), 6* (1966) 363; (b) M. Gouterman, in D. Dolphin (ed.), *The Porphyrins,* Vol. 3, Academic Press, New York, 1978, Ch. 1.
17 S. B. Brown and I. R. Lantze, *Biochem. J., 115* (1969) 279.
18 J. Owens and C. J. O'Connor, *Coord. Chem. Rev., 84* (1988) 1–45.
19 M. K. Kadish, in H. Gray and A. B. P. Lever (eds.), *Iron Porphyrins,* Elsevier, New York, 1983, pp. 161–245.
20 G. N. Lamar and M. Zorbrist, *J. Am. Chem. Soc., 100* (1978) 1944.
21 J. W. Owens, *Dissertation,* University of New Orleans, New Orleans, LA 70148, 1986.
22 D. K. Lavallee, *Coord. Chem. Rev., 61* (1985) 55.
23 A. Abragam and B. Bleaney, *Electron Paramagnetic Resonance of Transition Ions,* Clarendon, Oxford, 1970.
24 G. Palmer, in H. Gray and A. B. P. Lever (eds.), *Iron Porphyrins,* Elsevier, New York, 1983, ch. 2.

25 W. E. Blumberg, in A. Ehrenberg, B. G. Malstrom and T. Vanngard (eds.), *Magnetic Resonance in Biological Systems,* Pergamon, Oxford, 1967.
26 C. J. O'Connor, J. W. Owens and G. J. Hamilton, *Inorg. Chim. Acta, 93* (1984) 55.
27 M. Kotani, *Prog. Theor. Phys. (Kyoto Suppl.), 17* (1961) 4.
28 J. S. Griffith, *Biopolymers Symp., 1* (1964) 35.
29 R. G. Little, K. R. Dymock and J. Ibers, *J. Am. Chem. Soc., 97* (1975) 4532.
30 B. Shaanan, *J. Mol. Biol., 171* (1983) 31.
31 G. Harris, *Theor. Chim. Acta (Berlin), 10* (1968) 119.
32 (a) P. D. W. Boyd and T. D. Smith, *J. Chem. Phys., 56* (1972) 1253; (b) J. F. Boas, R. H. Dunhill, J. R. Pilbrow, R. C. Srivasta and T. D. Smith, *J. Chem. Soc. A,* (1969) 94.
33 W. S. Caughey, N. Sadasivan, H. Eberspaecher and W. Fuchsman, *Biochemistry, 8* (1969) 534; (b) I. Cohen, *J. Am. Chem. Soc., 91* (1969) 1980.
34 F. A. Walker, M. Lo and M. T. Ree, *J. Am. Chem. Soc., 98* (1976) 5552.